A mm-Wave Sensor for Remote Measurement of Moisture in Thin Paper Layers

A mm-wave Sensor for Remote Measurement of Moisture in Thin Paper Layers

Vessen Vassilev, Borys Stoew, Jakob Blomgren, and Gert Andersson

***Abstract*—We present the design and performance of a moisture sensor operating at 200 GHz for remote measurement of water content in paper. The system aims at industrial processes such as offset print and paper production. The moisture content in the paper is derived through an accurate measurement of the loss of a signal transmitted through the paper. The system is designed to achieve high accuracy in the measurement of the loss presented by the paper, not affected by 1/f or drift noise. The sensor is capable of resolving 0.005 dB loss achieving a moisture resolution of 0.1% for moisture content higher than 15%. The resolution can be improved if necessary in exchange for longer measurement times. The sensor is tested in offset print and paper production processes and measured values are compared to laboratory measured samples of the paper.**

***Index Terms*—Microwave sensors, Millimeter wave technology, Radiometers, Moisture control, Process control, Detectors, Schottky diodes, flicker noise.**

I. Introduction

WATER is a key parameter in offset print processes where the balance between water and ink is defining not only the quality of the print, but also the consumption of ink and spoilage of paper. The offset print industry is using four colors and, for two-sided print, the paper is run through eight offset stages where water and ink are applied resulting in graduate increase of the water in the paper. The water and ink flows are individually adjusted for each color, but the actual water content in the paper is not measured. Insufficient amount of water may cause unprinted areas of the paper to accept ink, while excessive water can wash away ink from printed areas. The water/ink balance is assessed by an operator and good quality print is associated with the operator skills and experience. Paper and press parameters, and their impact on the offset print quality has been examined in [1] emphasizing the need to measure the change in the amount of water in the paper during the print.

There are a number of commercially available sensors that can measure moisture content in paper layers. Infra-red (IR) sensors are based on measurement of absorption of infra-red radiation at specific wavelengths that are attenuated by water. In most of these sensors the radiation from a transmitter is reflected by the paper and its intensity is measured by a detector. In attempt to assess the ink-water balance in offset-print process in [1], water content has been measured using a commercial IR sensor. The result featured large variations (in some cases periodic) in the reading of the senor presumably caused by vibrations of the paper and/or density of the print. This class of sensors are therefore not considered appropriate for measurements in offset print process.

A second class of sensors giving a possibility to perform density independent moisture measurement are based on measurement of the complex dielectric constant by, for example, analyzing the quality factor of an open structure resonator where the water in the material is introducing loss in the cavity. Such resonators are either large in volume and/or require a contact with the paper, which is not acceptable for offset print process as it can tear the paper, which is running with a speed of up to 10 m/s. The water content in the paper is not evenly distributed along the cross direction and is affected by the density of the print. Therefore the only areas where sensing water can provide useful information to the operator is in the unprinted areas along the edge of the paper. A disadvantage of the resonator based sensors is that they do not provide sufficient spatial resolution and cannot resolve the white edges of the paper from the remaining areas.

A number of methods for mm-wave characterization of dielectric materials, including various interferometric techniques, have been demonstrated in the past [2]-[6]. Some of these systems require either scanning mirrors, or rotation of the dielectric sample. The specifics of such systems make them suitable for laboratory measurements, but not appropriate for online measurements in industrial processes. A valuable reference reading on the subject of industrial microwave sensors, with many examples is provided in [7].

In addition to better spatial resolution, moving from microwave to mm-waves gives a possibility do develop more compact sensors that can be incorporated into existing production processes. A quasioptical system for characterization of properties of materials in industrial process using measurement of transmitted and reflected from the sample beams is illustrated in [8]. Mapping moisture in a paper sample using THz time domain spectroscopy in laboratory environment is presented in [9]. Simultaneous measurement of

Manuscript received April 18, 2015; revised June 30, 2015; accepted July 16, 2015.

V. Vassilev, is with the Microwave Electronics Laboratory, Department of Microtechnology and Nanoscience at Chalmers University of Technology, SE 412 96, Göteborg, Sweden (e-mail: vessen.vassilev@ chalmers.se).

Borys Stoew, Jakob Blomgren, and Gert Andersson are with the Acreo Swedish ICT AB.

paper parameters such as moisture content and thickness using THz time domain spectroscopy are demonstrated in [10] where the paper parameter are extracted from the transmitted pulse profile with the help of effective medium models.

The focus in this work was to develop a simple sensor for measurement of moisture content in thin paper layers with resolution that is sufficiently high to detect moisture variations in offset print processes. The manuscript describes a prototype of a moisture sensor that measures the absorption of a transmitted continuous wave signal through the paper. Measuring the transmitted instead of the reflected signal contributes to measurement not affected by vibrations in the paper line. The wavelength of the signal is 1.5 mm making the measurement insensitive to structural composition of the paper while the beam is easily focused, and provides sufficient spatial resolution to be positioned at specific locations in the offset print process, for example on the white edges of the print.

In paper production processes the sensor can be used to scan and map the water content across the paper. The measurement method assumes that the basis weight of the paper is a constant and therefore variations in the absorption of the signal depend only on the water content. During the tests on a drying section of a paper-making machine presented in this manuscript, the basis weight of the paper was mapped using beta radiation and showed a constant mean value along the movement direction with variations on a small spatial scale, which are averaged away as the paper travels along the sensor.

The sensor has been tested in several occasions at both offset-print and on a drier stage of a paper production machines. The measurements performed in the offset print process reveal the required moisture resolution in order to register change by one-step in the water flow setting of the machine and thus help the operator to properly balance the water flow for each offset stage (color press) in the process. The achieved moisture resolution for specific measurement time of the sensor is given for both water and fountain solution, which is used instead of water in the offset print industry. For the tests on the drier, the sensor measurement is compared to data collected by a commercial resonant type of sensor. In addition samples of the paper were collected, the measured water content of both sensors is compared to laboratory measurement of the samples.

Uncertainty in the measurement due to standing waves is discussed and a solution to overcome the negative effects of components mismatch and optical misalignment is presented. In addition to the white noise, stability tests performed on the sensor reveal noise with *1/f* and $1/f^2$ spectrum. To avoid the negative effect of these low frequency noise on the moisture resolution, the system is periodically re-calibrated and thus the measured data contain only white noise that can be averaged to improve the amplitude and therefore moisture resolution at the expense of longer measurement time.

II. Sensor Design

The sensor system, shown in Fig. 1, consists of a transmitter illuminating the paper on one side and a receiver measuring the amplitude of the transmitted through signal. A voltage controlled oscillator (VCO) is generating the illumination signal, which is up converted to an RF frequency of about 200 GHz by a series of X2 and X6 multipliers. The X6 multiplier is an in house developed component and is described in detail in [11]. In order to avoid DC coupling between the detectors and the video amplifiers, the VCO signal is chopped by a switch at a rate of 1 kHz. To cancel the power variations of the 200 GHz signal, a waveguide 3 dB 90^0 hybrid is used to direct a part of the RF signal to a reference detector. The rest of the RF signal is applied to the transmitting horn and after reflected by a focusing mirror, the power is focused at a point close to a plane where the paper is positioned. The signal transmitted through the paper is attenuated in proportion to the water content. A second focusing mirror focuses the beam into the receiving horn antenna.

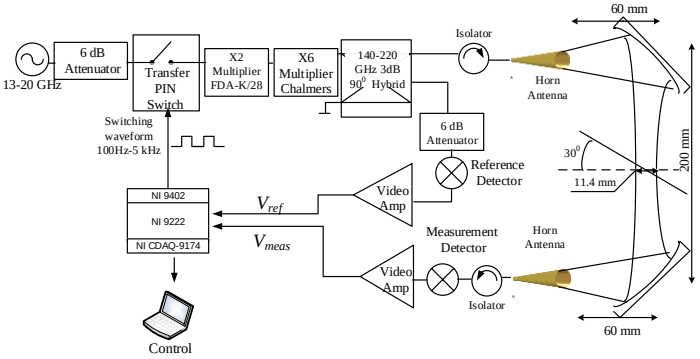

Fig. 1 A block diagram of the sensor. A pair of corrugated G-band (140-220 GHz) horns in combination with mirrors having focal length of 45 mm are used to transmit a probing signal through the paper.

Isolators are connected in front of both horn antennas in order to reduce standing waves in the optical path. For the same reason, the paper is positioned tilted such that reflected signal from the paper is directed away.

Low-noise zero-biased Schottky detectors are used to measure the signal power in both reference and measurement channels. The detected 1 kHz RF pulse envelope is amplified by video amplifiers and is applied to reference and measurement channels of an ADC where it is synchronously sampled and transmitted to a computer where the data processing is performed. The detection is synchronized by the 1 kHz switching waveform and the samples corresponding to the RF-signal ON and OFF states are summed and averaged for both reference and measurement channels.

Since the signal power in the reference and the measurement channel is not the same, the ratio of V_{meas}/V_{ref} is taken in a calibration measurement without a paper. The loss due to the paper is thus calculated by the ratio of V_{meas}/V_{ref} (with paper) to V_{meas}/V_{ref} (without paper). The measurement without the paper is further referred in the text as a calibration.

The measured total loss due to the paper includes both absorption within the paper and reflection loss. The measured total loss by the sensor is related to the water content in the paper by means of a look up table. A plot of such a relation is shown in Fig. 2 where a sample of the paper is moisturized and left drying while attenuation and weight of the sample are measured simultaneously. Attenuation vs. water content was measured for papers with different fiber contents, it was found

that the curves depend on the basis weight (thickness) of the paper, but not on the fiber content.

III. MOISTURE RESOLUTION

A relation between moisture content and attenuation of the transmitted signal is needed in order to measure the water content. The same relation is used to predict the moisture resolution, given a specific resolution in the measured signal attenuation. In this article the moisture content is defined as:

$$\psi = \frac{m_w}{m_w + m_p} \quad (1)$$

where m_w and m_p are the weight of the water present in the paper and the weight of the dry paper. Fig. 2 shows measured loss vs. moisture content for two cases: water and fountain solution, as used in offset print processes. The fountain solution is obtained by mixing tap water with additives in order to obtain appropriate pH balance, to protect machine parts against corrosion, and to avoid slime formations. The curves from Fig. 2 are obtained in laboratory tests by measuring the weight of a drying paper-sample while the attenuation of a transmitted signal is being measured simultaneously. The experimentally measured attenuation vs. moisture content is used as a lookup table for online measurements and also determines the achievable moisture resolution for a given amplitude resolution ΔA defined by the noise in the system.

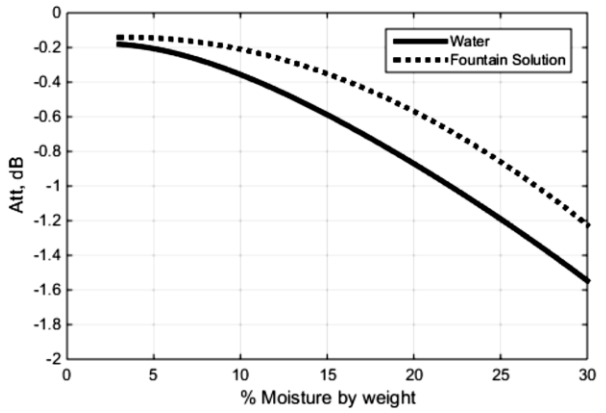

Fig. 2 Attenuation vs. water content in 45gr/m^2 paper in the case of moisture with water and with fountain solution, which is used in offset print processes.

A. Required amplitude resolution of the sensor

The experimental curves from Fig. 2 are used to calculate $dA/d\Psi$, the moisture resolution $\Delta\Psi$ given by $\Delta A/dA/d\Psi$ is shown in Fig. 3 for $\Delta A=0.005dB$ where ΔA is the amplitude resolution achievable by the sensor.

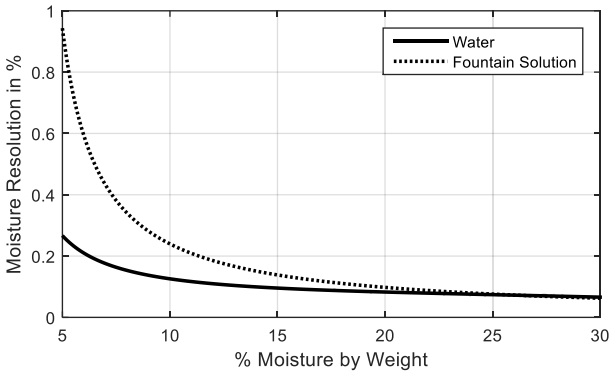

Fig. 3 Expected moisture resolution for amplitude resolution of ΔA=0.005dB.

Factors limiting the resolution of the system and measures that are taken to minimize ΔA are discussed in the section below.

IV. AMPLITUDE ACCURACY

The moisture resolution of the sensor is defined by the accuracy of the amplitude measurement. There are two factors limiting the accuracy of amplitude measurements. The first one is related to miss-match between the transmitter and the receiver giving rise to a standing wave pattern between the antennas; the second one is caused by noise in the detectors.

A. Standing waves (SW)

Non perfect match between ports of a two-port network and misalignment of the optical components result in a frequency dependent transmission coefficient. The amplitude and the period of the standing wave pattern is defined by:

$$\Delta A = 20 \cdot \log(1 \pm \Gamma_S \Gamma_L); \quad \Delta f = \frac{v}{2 \cdot L} \quad (2)$$

where Γ_S, Γ_L are reflection coefficients at the ports of the network, L is the separation between the ports and v is the speed of the wave.

The attenuation is measured as a ratio of the power transmitted through the paper to the corresponding power without the paper. For a measurement of transmission, the presence of SW will affect the accuracy of the measurement, as the presence of the paper and water will shift the SW pattern. The resulting error is impossible to compensate if the measurement is performed at a single frequency. The maximum value of this error, or the uncertainty is given by eq. (2).

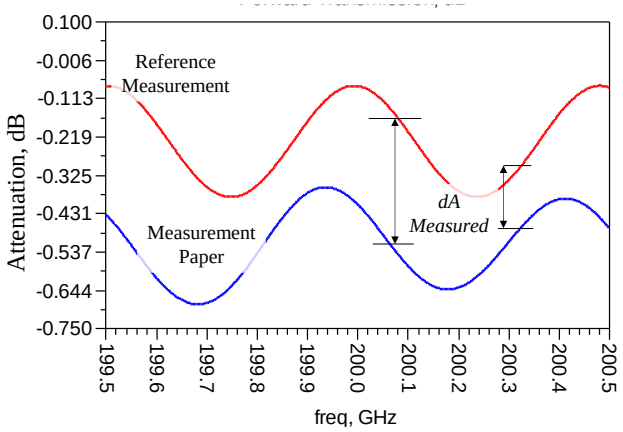

Fig. 4 Illustration of a standing wave pattern for antennas separated at 320 mm and return loss of Γ_S=-15 dB, Γ_L=-20 dB without and with the paper. When the paper is inserted, the SW pattern will shift in frequency depending on the paper thickness (60 um in this case) and water content, which limit the accuracy of the measurement if the measurement is performed at one frequency only. Measurements at different frequencies will give different values for the attenuation. The presence of the paper will also change the SW period compared to the reference measurement, but when measurements at frequencies covering several SW periods are averaged, the effect of the different SW periods will be insignificant.

As shown in Fig. 1, a pair of isolators are used to improve the SW between the antennas, the return loss of these components is -15 dB and -20 dB at 200 GHz. The calculated SW pattern in the transmission is shown in Fig. 4 without and with paper. To overcome the negative effect of the SW, the measurement is performed at a number of frequencies covering, ideally, an integer number of SW periods. In the simplest case of two planes of reflections, the SW period is defined by the distance between the planes (eq. 2) i.e. the separation between the transmitter and the receiver. Other sources of reflections may occur as result of optical misalignments that may additionally modify the SW pattern. The sensor performs measurement at 25 frequency points covering approximately three periods of SW. Each moisture reading is thus an averaged value of all frequency points measured. Additional advantage of this approach is that the VCO can be operated without phase locking control.

B. Noise

One way of performing a measurement is to take a calibration measurement without the presence of paper and then refer a series of measurements with the paper to this initial calibration, this measurement sequence is illustrated in eq. (3).

$$\overbrace{\text{CAL}}^{\text{OFF Paper}}, \overbrace{\text{Meas.1, Meas.2, Meas.3, } \ldots\ldots}^{\text{ON Paper}} \qquad (3)$$
$$\text{Point } 1 = \frac{\text{Meas.1}}{\text{CAL}}, \text{Point } 2 = \frac{\text{Meas. 2}}{\text{CAL}}, \ldots..$$

While such a measurement is beneficial in terms of speed it has the disadvantage of being limited by low-frequency noise for the measurement points taken later than a certain time after the calibration (CAL) measurement is performed. Noise in this measurement can be characterized by taking a series of measurements without the presence of a paper. Ideally the result should give a constant ratio of one. Such a series of measurement points is presented in Fig. 5 where a measurement points is logged each 0.28s while the actual measurement time is 45 ms.

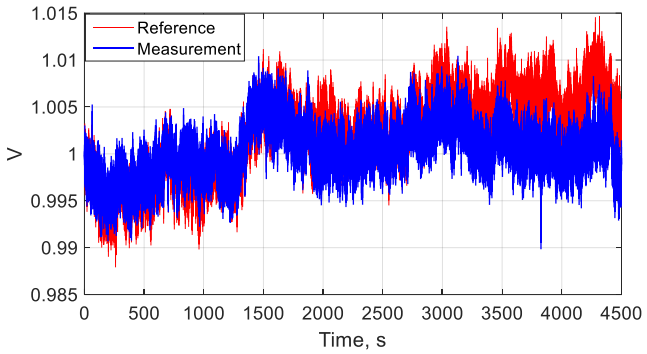

Fig. 5 The normalized detected voltages for the reference and the measurement channels without presence of a paper. The variations in the signal power are registered by both channels and does not affect the the ratio of both channels. However, changes in responsitivity of the detectors is also visible and can not be compensated.

The ratio of this series is shown in Fig. 6 indicating that the measurement is affected by drift due to unbalanced change of the responsivity of the measurement and the reference detectors, most likely caused by changing temperature difference.

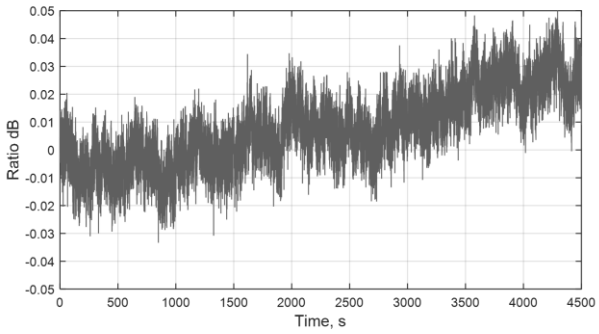

Fig. 6 Ratio of reference and measurement channels from Fig. 5. All measurement points are referred to the initial calibration at time 0 as shown in eq. (3). The ratio is close to 0 dB only for the first data points.

The spectrum content of the noise and the balance between the noise contributors in the measurement can be evaluated with the help of the Allan variance, first introduced in [12]. A plot of the Allan variance as a function of the number of the averaged measurement-points, for the data series in Fig. 6, is given in Fig. 7. The plot indicates that white noise dominates the measurement only over the first 10 measurement points (or about 3 seconds). On time scale longer than 12s (corresponding to 40 measurement points), noise featuring $1/f^2$ spectrum limits the accuracy of the measurement.

The square root of the Allan variance from Fig. 7 has a meaning of $\Delta V/V_{det}$ where ΔV is the noise component of the detected ratio from Fig. 6. Since this measurement is carried without a paper $V_{det}=1$ and $\Delta V/V_{det}$ corresponds to the noise-to-signal ratio of the measurement. The uncertainty of the power ratio measurement in dB is also indicated for no averaging and at the minimum of the plot where the low frequency noise becomes dominant.

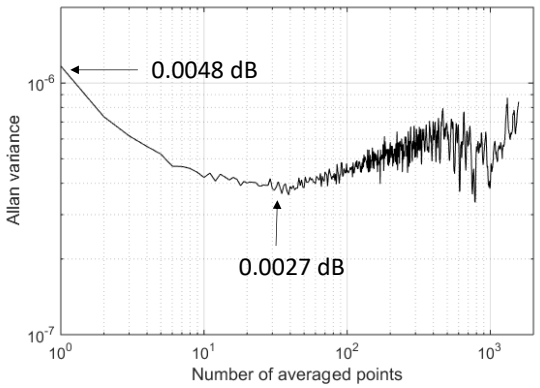

Fig. 7 Allan variance plot of a series of 16k measurements of attenuation without presence of a paper from Fig. 6. The time interval between the data points is 280ms, the actual measurement (sampling) time is 48 ms per point.

A properly designed measurement would be limited by a white noise only allowing to achieve any resolution by averaging the required number of white noise limited measurement points. The plot in Fig. 7 suggests that if amplitude resolution better than ±0.0027 dB is required the system needs to be recalibrated each couple of seconds by removing the paper from the sensor and making a new calibration measurement. Such a measurement sequence with accuracy only limited by white noise can be further averaged to achieve resolution, which scales with $1/(N)^{0.5}$ where N is the number of averaged samples.

The re-calibration functionality was implemented by mounting the sensor on a linear stage driven by a motor. The measurement sequence is illustrated in eq. (4):

$$\overbrace{\text{CAL.1}}^{\text{OFF Paper}},\overbrace{\text{Meas.1}}^{\text{ON Paper}},\overbrace{\text{CAL.2}}^{\text{OFF Paper}},\overbrace{\text{Meas.2}}^{\text{ON Paper}},\ldots..$$
$$\text{Point } 1=\frac{\text{Meas.1}}{\text{CAL.1}},\ \text{Point } 2=\frac{\text{Meas.2}}{\text{CAL.2}},\ldots.. \quad (4)$$

The measurement of the attenuation in the absence of a paper sample using a re-calibration for each measurement point as described above was repeated and the result is presented in Fig. 8. The Allan variance plot of this measurement is given in Fig. 9 and shows no remains of noise other than white noise. The drawback of this implementation is the extra time needed to position the sensor at ON and OFF the paper, making the measurement slower.

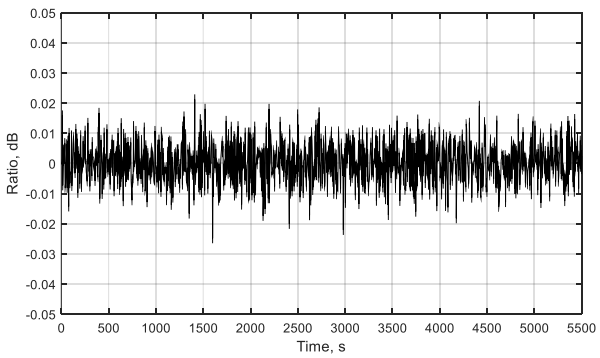

Fig. 8 A sequence of 1352 measurements of attenuation without the presence of the paper after implementing the recalibration. A calibration is performed for each data point by removing the sensor from the paper according to eq. (4).

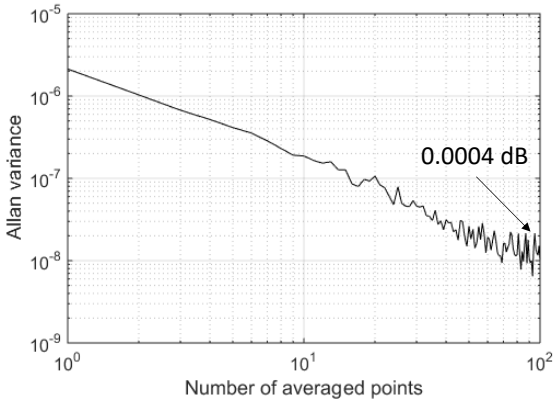

Fig. 9 Allan variance of the data from Fig. 8 with re-calibration implemented according to eq. (4), the amplitude resolution in dB achieved after averaging 100 measurement points is also indicated. The time interval between the points is as in Fig. 7 plus the time required to position the sensor between "ON" and "OFF", which is of the order of 1sec.

V. Measurements

This section summarizes two measurements, at an offset-print plant before the re-calibration functionality was implemented eq. (3) and on a dryer stage of a paper making machine with the re-calibration implemented, as described above in eq. (4).

A. *Offset print*

The sensor was mounted several meters after the offset-print stage where the last color is applied [13] and the beam was focused at the unprinted margin on the edge of the paper, as illustrated in Fig. 10. The water inflow was changed by the operator while the sensor was measuring continuously.

Fig. 10 Sensor location in the offset process. The beam is focused on the white strip at the edge of the paper.

At the beginning of each measurement sequence the sensor is taken away from the paper to perform a calibration measurement to which the measurement of the paper are referred to, according to eq. (3). An example of measurement sequence, obtained with the setup from Fig. 10, is shown in Fig. 11 for three different machine settings of the water flow (applies for all 8 colors).

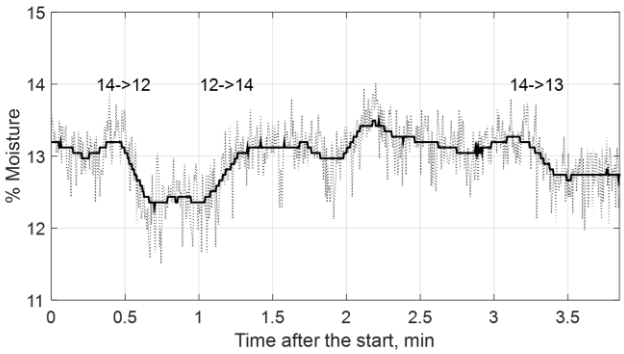

Fig. 11 Measurement series of data in the offset print process. Calibration measurement without a paper was performed only at the start, at time 0. The numbers above the trace indicate times when the water flow settings were changed, 25 sec after the start the water flow was decreased for all colors by 2 units, at about 1 min after the start the setting was restored to 14 units. The dotted line shows raw measurement data with time interval between the points 0.3 s. The solid line shows smoothed data with smoothing window of 50 points.

The measurements showed that the offset process increases the water content from about 6% (at the input of the machine) to about 14 % after the last color is printed. This corresponds to about 1% increase per color and moisture resolution of about 0.05% is required if the sensor is to resolve one step in the water flow setting per color (water flow setting is on a scale 1-15 units for each color). The amplitude resolution of this measurement is as indicated from the Allan variance plot in Fig. 7. For a measurement sequence of the order of minutes where each data point is referred to the calibration measurement at time 0 the amplitude accuracy is expected to be ±0.005 dB. The expected moisture resolution can be obtained from Fig. 3, for the case of fountain solution it is of the order of ±0.2 %.

This result suggested that the sensor accuracy in the attenuation measurement is not sufficient to help to properly balance water flow setting among the eight colors. This conclusion led to the design of a mechanical structure that allows for a calibration for each data point as shown in eq. (4), i.e. the sensor is taken away from the paper, the power in both measurement and reference channel is measured and after positioning the sensor over the paper the same measurement is repeated. After this upgrade the sensor was tested again, this time in a paper production process described below. The amplitude resolution after this upgrade is indicated in Fig. 9.

B. Drier stage of a paper making machine

The sensor was installed at the output of a drying section of a paper production machine [14]. The drying stage consists of a number of heated cylinders coming into contact with the paper. Data were collected while the moisture content in the paper was varied by changing the speed of the drier or the temperature of the drying cylinders. Data were simultaneously taken with a microwave resonance sensor which was in contact with the paper in the vicinity to the mm-wave sensor. Papers with different basis weight and fiber content, as indicated in Table 1, were measured by both sensors. In addition, samples from the paper were collected for off-line laboratory measurement which are used as a reference.

	A	*B*	*C*
Basis weight, gr/m^2	61,3	51	64.3
Approximate thickness, µm	94	78	99
Fiber type 1 content, %	80	60	60
Fiber type 2 content, %	20	40	40

Table 1 A list of the papers measured. Different combinations of fiber content and basis weight were tested.

Attenuation vs. water content curves, similar to the one presented in Fig. 2 were measured for each type of paper. The curves do not suggest dependence on the fiber content, but only on the basis weight.

In the measurement presented in Fig. 12 to, Fig. 14, the drying cylinders are kept at constant temperature of 40 ºC while the speed of the dryer was varied. Higher speed results in higher water content. However, changing the speed of the dryer does not result in instantaneous change in the water content since it takes time for the paper, which is already in the machine to come out and be replaced by a paper dried entirely with the "new" speed throughout the entire machine.

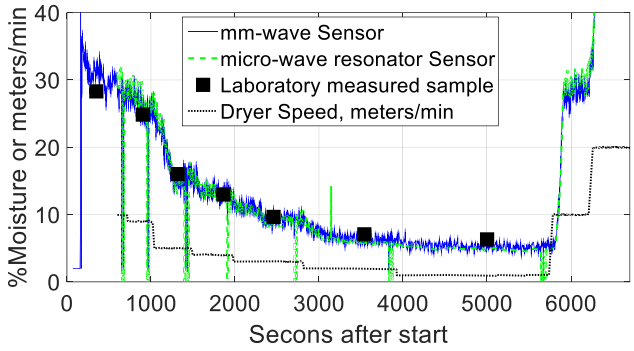

Fig. 12 Measured moisture content of paper A. Drying cylinders are kept at constant temperature of 40 ºC. Squares indicate the moisture content by laboratory measurement of samples of the paper.

Fig. 12 to Fig. 14 show raw data with time interval of 1s for the microwave resonator and 3.4s for the mm-wave sensor. The actual measurement time for the mm-wave sensor is about 45 ms, the rest of the time is spent on moving the sensor to ON and OFF positions and signal processing.

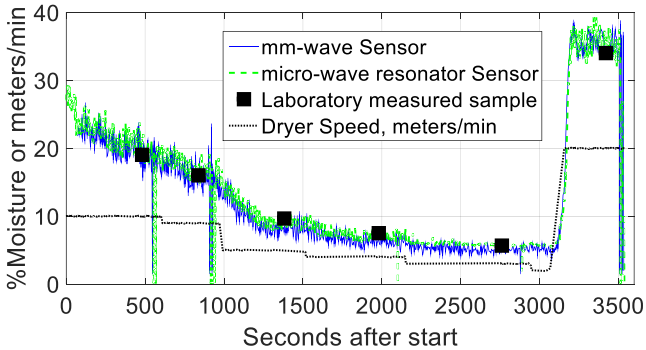

Fig. 13 Measured moisture content of paper B. Drying cylinders are kept at constant temperature of 40 ºC. Squares indicate the moisture content by laboratory measurement of samples of the paper.

Improving the speed of the mm-wave sensor would contribute to better accuracy as more data points can be

collected and averaged over the same time interval. Running the measured data for "paper A" through a smoothing window reveal that both sensors underestimate the laboratory measured moisture by 1% at low (6%) moisture content. Both sensors agree well with the laboratory measured samples for moisture contents between 10 and 25%.

For papers "B" and "C" the discrepancy between the reading of both sensors and the laboratory measured samples is less than 1% for most of the samples.

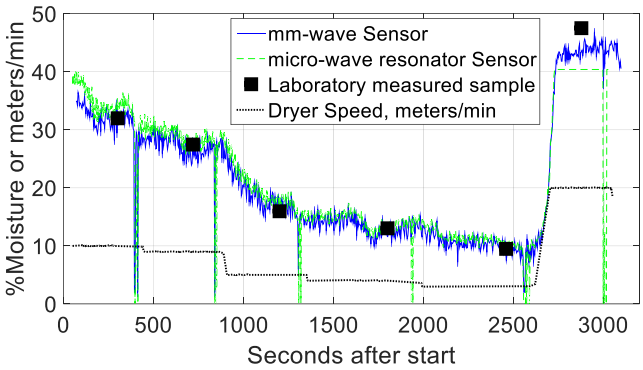

Fig. 14 Measured moisture content of paper C. Drying cylinders are kept at constant temperature of 40 ºC. Squares indicate the moisture content by laboratory measurement of samples of the paper.

Attenuation vs. water content curves used in these measurements were obtained for paper drying at room temperature. In order to test how much the reading of the sensors are affected by the paper temperature, the temperature of the dryer was increased to 80 ºC in the last measurement presented in Fig. 15. The cylinders reached 80 ºC after about 300 seconds after the start. However, the paper cools down to about 38 ^{0}C by the time it travels between the last cylinder and the point where the sensor is placed, which is still about 10 ^{0}C higher than the measurements from Fig. 12-Fig. 14.

Since the dielectric constant of water is temperature dependent, temperature settings of the drying cylinders will cause a change in the paper temperature at the output of the drier. Unless accounted for, measurement of the water content at elevated temperature will overestimate the measured water content. To determine the influence of temperature to the accuracy of the measurement, we calculate the transmitted power through a dielectric slab in air, as described in [4], considering the effective dielectric constant of the paper-water mixture, the thickness of the paper sample, polarization and angle of incidence. To calculate the effective dielectric constant of the mixture: paper plus water, we use the Bruggeman's formula [15], [16]. The formula requires knowledge of the dielectric constants of both paper and water. The temperature dependent water dielectric constant at 200 GHz is extracted from a model presented in [17]. A good fit to the measured data is obtained for paper dielectric constant of $\mathrm{Re}(\varepsilon_p)=2.25$ and $\mathrm{Im}(\varepsilon_p)=0.0018$, which is in a good agreement with measurements of the refractive index of paper presented in [15] and [18]. A summary of these calculations is presented in tables 2 and 3 for 2 different moisture levels.

Paper temperature, ^{0}C	*Att, dB*	*Extra Att, dB*	*Offset, %*
20	0.5437	0	0
30	0.5692	0.025	+0.51
40	0.5804	0.037	+0.76

Table 2 Offset in the measured moisture content for samples at 30 ^{0}C and 40 ^{0}C when a lookup table obtained at 20 ^{0}C is used. Values are calculated for 9% of moisture. The water dielectric constant at 200 GHz as extracted from [17] is: 20 ^{0}C (5.73-j7.0); 30 ^{0}C (5.89-j8.19); 40 ^{0}C (6.2-j9.18).

The tables illustrate how much the water content is overestimated if the attenuation vs. water content lookup table is measured at room temperature, while the online measurements are performed at higher temperatures.

Paper temperature, ^{0}C	*Att, dB*	*Extra Att, dB*	*Offset, %*
20	1.757	0	0
30	1.914	0.16	+1.6
40	2.022	0.26	+2.6

Table 3 Offset in the measured moisture content for samples at 30 ^{0}C and 40 ^{0}C when a lookup table obtained at 20 ^{0}C is used. Values are calculated for 25% of moisture.

The result from tables 2 and 3 suggest that temperature of the paper-water mixture should be considered if the absolute moisture level is important. Increased temperature will result in overestimate of the actual water content especially at higher moisture contents. This is also visible in Fig. 15 where for level of 25 % both sensors measure higher moisture value than the laboratory measured sample.

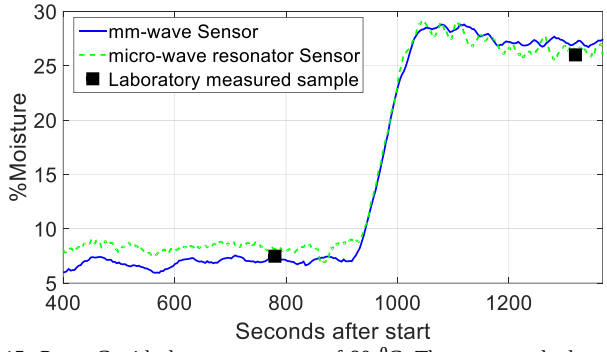

Fig. 15 Paper C with dryer temperature of 80 ^{0}C. The paper cools down to about 38 ^{0}C at the point where the sensor is placed, which is still about 10 ^{0}C higher than the measurements from Fig. 12-Fig. 14. The figure shows smoothed data with a window of 20 points.

The variations in the measured moisture content presented in Fig. 12 - Fig. 14 are larger than the expected moisture resolution indicated in Fig. 3. The likely cause for the variations is in the fact that there are two heaters per cylinder, which produce certain temperature gradient over one period of rotation of the cylinders having a diameter of 0.8m. Fig. 16 shows a selection of data from Fig. 13 indicating the timescale of the variations. The fast variations period of 4s, matches the dryer speed of

20m/min. Another source of longer period variations most likely comes from the control system stabilizing the temperature of the heaters.

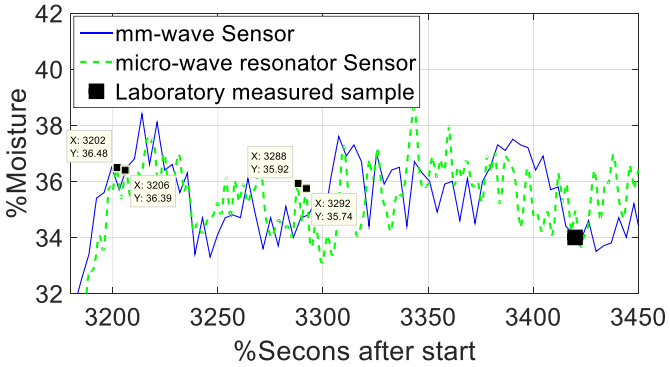

Fig. 16 A zoomed form of the data for paper B presented in Fig. 13. Variations in the measured moisture content show an obvious correlation between the readings of both sensors, despite the fact that they are not sensing the same areas of the paper. We believe that these variations are not due to noise, but are real moisture variations caused by a temperature gradient in the drying cylinders.

Another observation supporting the statement that the observed moisture variations are real and not result of noise is the fact that the amplitude of the variations decrease as the paper is dried to about 5-6%, this is clearly visible in Fig. 12 to Fig. 14.

In order to verify the assumption that the paper basis weight (BW) does not vary along the direction of movement, a sample of paper B was measured off-line using a beta radiograph. The result is shown in Fig. 17 indicating a constant mean value of the BW along the length of the paper. This measurement, and the good agreement between the moisture values measured by the mm-wave sensor and the laboratory measurements of the paper samples suggest that the mean value of the BW does not vary within a paper roll.

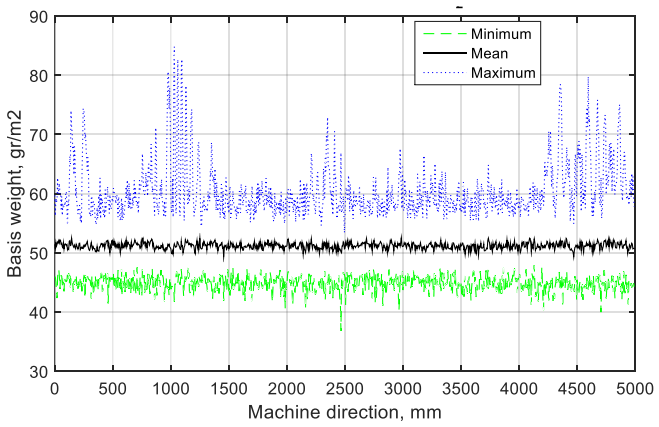

Fig. 17 Plot of the measured minimum, maximum and mean values of the BW of paper B over the transverse direction (width of the paper) vs. longitudinal dimension (Machine Direction, MD). The large variation in the value for the maximum basis weight is due to a fold (a stripe of double layer), which appeared during the loading of the sample.

VI. Conclusion

This article demonstrates the implementation of a moisture sensor for contactless measurement of water content of papers with known basis weight.

Tests conducted in an industrial offset print process suggest that a moisture resolution of better than 0.05% is required if the sensor is to resolve one step in the water flow setting per color. In order to achieve this requirement the system was upgraded with a moving stage allowing to re-calibrate the sensor by taking a reference measurement without the paper for each data point and therefore removing low-frequency noise from the measurements. Because of the limited time in the project we could not repeat the tests in offset print process after the upgrade. The sensor was tested instead on the drying stage in a paper production process.

A number of papers were tested in different drying conditions where the speed and drying temperature are varied. Data are taken simultaneously with two sensors: a microwave resonator sensor, and the mm-wave sensor presented in this article. While the microwave sensor requires a contact with the paper, the mm-wave sensor measures the moisture remotely. Both sensors give similar readings, which also agree well with laboratory measurements of a number of paper samples taken during the measurement. The observed variations in the measured moisture content for higher concentrations are caused by actual moisture variations. The mm-wave sensor presented in this article measures the moisture content over an area of about 4cm^2 and in the future can be used to scan and map the moisture profile across the paper path.

Acknowledgment

The authors would like to thank Bengt Larsson (V-Tab Hisings Backa) and Fredrik Sköld (V-Tab Halmstad) for their help during testing the sensor in offset print process, Andrew Horvath, Luis Carlos Felix Tapia, Marco Lucisano and Karin Athley for they support during the measurement campaign at the paper making installation at Innventia. The authors would also like to thank the reviewers of the manuscript for their valuable comments. This work is supported by the Swedish innovation agency VINNOVA.

References

[1] J. Lundström, A. Verikas, E. Tullander, B. Larsson, ”Assessing, exploring, and monitoring quality of offset colour prints”, *Measurement*, 46 (2013), 1427–1441.

[2] M. N. Afsar, J. R. Birch, R. N. Clarke, G. W. Chantry, “The measurement of the properties of materials”, *Proceedings of the IEEE*, Vol.:74 , Issue: 1, 1986.

[3] Afsar, M.N., “Dielectric Measurements of Millimeter-Wave Materials”, *IEEE Transactions on Microwave Theory and Techniques*, Vol.: MTT-32 , Issue: 12, December 1984.

[4] F. Shimabukuru, “A quasioptical method for measuring the complex permittivity of materials”, *IEEE Transactions on Microwave Theory and Techniques*, Vol. MTT-32, July 1984.

[5] Stumper, U., “Six-port and four-port reflectometers for complex permittivity measurements at submillimeter wavelengths”, *IEEE Transactions on Microwave Theory and Techniques*, Vol.: 37 , Issue: 1, January 1989.

[6] W. Hoppe, W. Meyer, W. M. Schilz, “Density-Independent Moisture Metering in Fibrous Materials Using a Double-Cutoff Gunn Oscillator”, *IEEE Transactions on Microwave Theory and Techniques*, Vol.:28 , Issue: 12, December 1980.

[7] Ebbe G. Nyfors, Pertti Vainikainen, ”Industrial Microwave Sensors”, Artech House Microwave Library, December 1989.

[8] P. Goldsmith, “Quasioptical Systems”, IEEE Press, ISBN: 0-7803-3439-6.

[9] D. Banerjee, W. von Spiegel, M. D. Thomson, S. Schabel, H. G. Roskos, " Diagnosing water content in paper by terahertz radiation*", Optics Express*, Vol. 16, Issue 12, pp. 9060-9066 (2008).
[10] Payam Mousavi, "Material composition analysis using time-domain terahertz spectroscopy", a PhD dissertation, Department of Physics, Faculty of Science Simon Fraser University, 2014, available at. http://summit.sfu.ca/item/14105.
[11] V. Vassilev, N. Wadefalk, R. Kozhuharov, M. Abbasi, H. Zirath, T. Pellikka, A. Emrich, I. Kallfass, A. Leuther, "MMIC-based receivers for mm-wave radiometry", *35th International Conference on Infrared Millimeter and Terahertz Waves (IRMMW-THz)*, 2010.
[12] David W. Allan, "Statistics of Atomic Frequency Standards", Proceedings of the IEEE, Vol. 54, No.2 Feb 1966.
[13] V-TAB Backa Exportgatan 2-4, 422 46 Hisings Backa, Sweden
[14] Innventia AB, Drottning Kristinas väg 61, Stockholm, Sweden
[15] Payam Mousavi, Frank Haran, David Jez, Fadil Santosa, and John Steven Dodge, "Simultaneous composition and thickness measurement of paper using terahertz time-domain spectroscopy", *Optical Society of America*, Vol. 48, Issue 33, 2009.
[16] T. C. Choy, "Effective Medium Theory: Principles and Applications", *The International Series of Monographs on Physics (Book 102), Oxford University Press*, 1999.
[17] Thomas Meissner and Frank J. Wentz, "The Complex Dielectric Constant of Pure and Sea Water From Microwave Satellite Observations", *IEEE Transactions on Geoscience and Remote Sensing*, Vol. 42, No. 9, Sept. 2004. Online tool available at: http://www.random-science-tools.com/electronics/water_dielectric.htm
[18] Hattori, T., Kumon, H. Tamazumi, H. "Terahertz spectroscopic characterization of paper", *35th International Conference on Infrared Millimeter and Terahertz Waves* (IRMMW-THz), 2010.

Vessen Vassilev received M. Sc degrees in "Radio Communications" from the Sofia Technical University in '95, and in "Digital Communications" from Chalmers University of Technology in '98. In 2003 he received his PhD degree from the department of "Radio and Space Science" at Chalmers University. Between 1998 and 2008 he has been working with the development of mm-wave receivers for applications in radio astronomy and space sciences. Instruments designed by him are currently in operation at the Atacama Pathfinder Experiment (APEX) telescope and at the Onsala Space Observatory. Since 2008 he has been with the Microwave Electronics Laboratory at the Department of Microtechnology and Nanoscience at Chalmers. His current interests are in the development mm-wavelength sensors based on MMIC technologies.

Borys Stoew has been with ACREO AB since 2005 working on digital system design. In particular, he specializes in digital control loops and signal processing using FPGAs as a platform for ASIC development. He received his PhD from Chalmers in 2004 in the field of microwave remote sensing using radiometry and GPS. He holds a MSc. of electrical engineering from the Digital communications program at Chalmers.

Dr. Jakob Blomgren received his M.Sc. in Engineering Physics 1995 and his Ph.D. in Physics 2001 from Chalmers University of Technology in Göteborg, Sweden. He joined Acreo in 2001 where he works both as a research scientist and project manager in the area of magnetic sensors, magnetoelastic resonance sensors, humidity and moisture sensors, wireless sensors and applications of wireless sensor networks. He has written over 15 papers in peer-reviewed international journals in the field of sensitive magnetic sensing and magnetic nanostructures and he is also co-inventor of 5 patents in the field of magnetic sensing.

Gert I. Andersson, MSc.EE, Ph. D, Associate Professor. His doctoral studies concerned the influence of process-induced defects on electrical properties of silicon junctions. After the doctoral studies his research has focused on MEMS sensors, especially inertial sensors accelerometers and gyros. First, for a period of six years at the department of Solid-State Electronics at Chalmers University of Technology as researcher, lecture, group leader and laboratory manager. In January 1999, he joined the new founded Imego institute. There he has had a central role in building-up the institute that now is merged with Acreo AB. His publication list includes more than 50 technical publications (> 500 citations), approximate 10 patent portfolios with more than 30 granted and pending patents. He has successfully managed to transfer his own research results to commercial products as one of the inventors to the Butterfly-gyro, a MEMS gyro for automotive and high performance professional applications.